On cell surface deformation during an action potential

Christian Fillafer[a], Matan Mussel[a,b], Julia Muchowski[a], Matthias F. Schneider[a]

[a]Technical University of Dortmund
Department of Physics
44227 Dortmund
Germany

[b]University of Augsburg
Department of Physics
86159 Augsburg
Germany

[1]**Address correspondence to:** Dr. Matthias Schneider
Technische Universität Dortmund
Medizinische und Biologische Physik
Otto-Hahn-Str. 4
44227 Dortmund
tel: +49-231-755-4139
email: matthias-f.schneider@tu-dortmund.de

Abstract

Action potentials (AP) are considered to be electrical phenomena. However, non-electrical changes at the cell surface have been reported and resulted in contradictions with the classical theory. The evidence presented herein corroborates that an AP is not a purely electrical phenomenon. It is demonstrated that excitation of plant cells (*Chara braunii* internodes) is accompanied by out-of-plane displacements of the cell surface in the micrometer range (~1–10 μm). The onset of cellular deformation coincides with the depolarization phase of the AP. The mechanical pulse *(i)* propagates with the same velocity as the electrical pulse (within experimental accuracy; ~10 mm s^{-1}), *(ii)* is reversible, *(iii)* in most cases of biphasic nature (109 out of 152 experiments) and *(iv)* presumably independent of actin-myosin-motility. The existence of transient mechanical changes in the cell cortex is confirmed by micropipette aspiration experiments. A theoretical analysis demonstrates that this observation can be explained by a reversible change in the mechanical properties of the cell surface (transmembrane pressure, surface tension and bending rigidity). Taken together, these findings contribute to the ongoing debate about the physical nature of cellular excitability.

Significance Statement

Ever since the controversy between Galvani and Volta in the early 19th century, excitation processes in cells and tissues have been considered to be of an electrical nature. Several lines of evidence (see *e.g.* (1, 2)) suggest that this conclusion was premature. It is demonstrated herein that an action potential is associated with a significant deformation of the cell; *i.e.,* a change in its mechanical properties. These observations are not predicted by the present electrical theory and demonstrate the relevance and importance of additional macroscopic variables for understanding cellular excitation.

Introduction

Action potentials (AP) are intriguing phenomena that appear in many biological systems (neurons, myocytes, excitable plant cells, etc.). For a long time, it has been believed that these pulses are of an electrical nature. The mathematical description of APs was based on the view that the excitable membrane can be fully represented by an equivalent circuit (3). However, this approach has come under substantial criticism. The debate has been stirred up by Tasaki (4–12) and has been extended mainly through the works of Kaufmann (2, 13) and Heimburg (1, 14). One of the central points of criticism of the electrical framework is that it neither contains nor predicts non-electrical manifestations of the AP. These pulse components, however, exist and include optical (4), thermal (15), magnetic (16) as well as mechanical (5–8, 17) changes at the cell surface. The latter have been studied with a variety of highly sensitive techniques (piezoelectric benders, interferometry, AFM). At first, the inherently soft nature of nervous tissue preparations combined with the sheer minuteness of the movements posed difficulties and led to varying results (5–7, 17). Nevertheless, more recent studies are in agreement and indicate that the mechanical pulse in cylindrical axons is of biphasic nature with expansion followed by contraction (~1–10 nm) (8, 18). In parallel, there exists a biphasic intracellular pressure wave (18). Intriguingly, neither the mechanism behind the mechanical pulse component nor its relation to the electrical events are currently understood. Aside from APs in axons, other excitation phenomena in biology are also associated with mechanical changes. Deformations were reported, for instance, in muscle cells (19) as well as during spreading depression waves in cortical tissue (20). It must be of central interest to investigate if these phenomena can be explained by a unified theory.

While there exists firm evidence that an AP is *not only* an electrical *but also* a mechanical pulse, several open questions remain. Even in well-cleaned axons the cell surface is covered by extracellular matrix and Schwann cells (9). This makes it difficult to observe and study the excitable membrane directly. Moreover, if this sheath is stiffer than the underlying cell membrane it will lead to significant attenuation of mechanical signals. Thus, the actual mechanical changes during an AP may be larger than anticipated. Herein, we attempt to contribute to these open problems. Mechanical changes are investigated during AP propagation in plant cells. Internodes from *Charophytes* are well suited for this purpose. These cells are large (diameter ~0.5—1 mm; length ~1—15 cm), easy to handle and have a long-standing history in excitable cell research (21, 22). In *Charophytes*, comparatively large radial and axial deformations have been reported during an AP (~100 nm (6, 23)). As in the case of axons, the mechanical pulse is biphasic and consists of expansion followed by contraction (24). Herein, we demonstrate that "freeing" the excitable membrane from the constraints of the plant cell wall reveals even larger surface displacements in the micrometer range. A theoretical analysis indicates that these deformations during an AP are due to reversible changes in the mechanical properties of the cell surface (transmembrane pressure, surface tension, bending rigidity).

Results

Cell surface deformations during an AP. In a native *Chara* cell, the plasma membrane is tightly pressed against the cell wall by a turgor pressure ($\sim 6 \cdot 10^5$ N m^{-2} (25)) (Fig. 1a). However, by changing the extracellular osmotic pressure it was possible to progressively reduce turgor until the plasma membrane detached from the cellulose sheath – a process known as plasmolysis (Fig. 1b) (26, 27). During this procedure, the protoplast did not retract uniformly. In certain regions (*e.g.,* at the nodes) the membrane still adhered to the cell wall whereas in other areas it detached entirely. Initially, the shape of a plasmolysed cell was irregularly wavy. As time progressed, the protoplast equilibrated, assumed an unduloid-like form, and eventually fragmented[*].
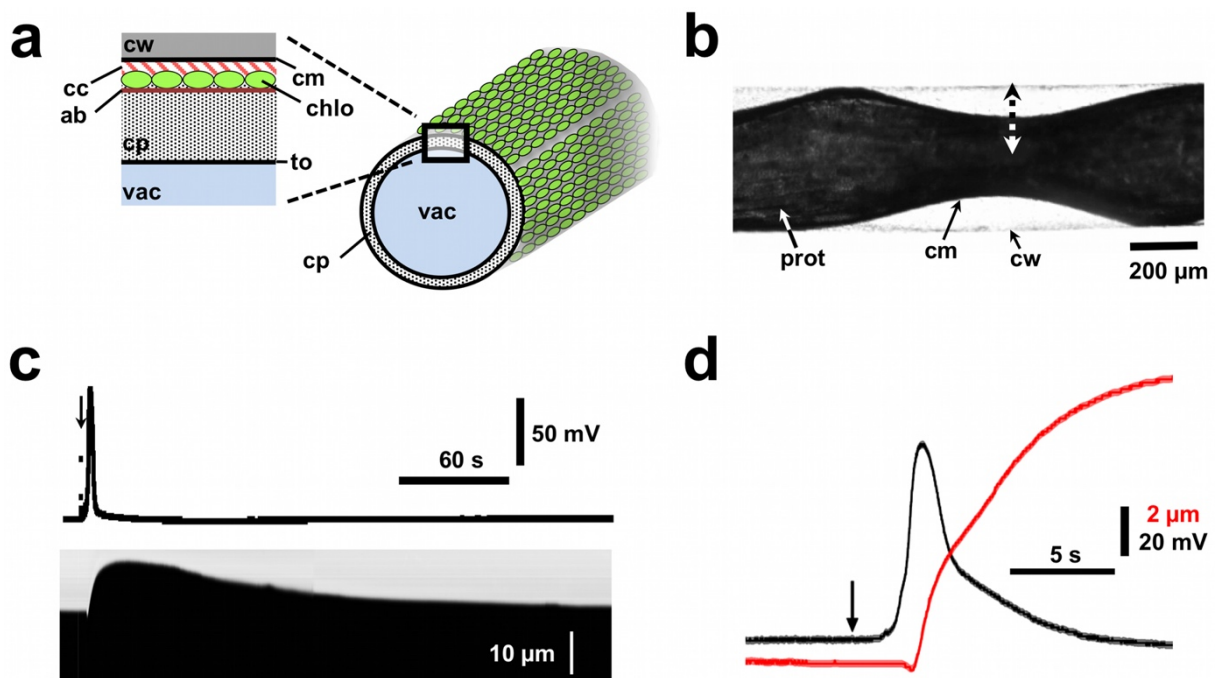
Figure 1. Cell surface deflection during an action potential (AP). (a) In *Chara*, the cytoplasm (cp) is marginalized by the tonoplast (*to*)-covered vacuole (*vac*). The cellular cortex consists of the cell wall (*cw*), cell membrane (*cm*), cortical cytoskeleton (*cc*), chloroplasts (*chlo*) and subcortical actin bundles (*ab*) (see (28)). **(b)** When turgor was reduced by changing the external osmotic pressure, *cm* separated from *cw*. Deflections (dashed arrow) of the projection edge of the protoplast surface (*prot*) were tracked by light microscopy. **(c)** Upon excitation of an AP the cell surface underwent a biphasic, reversible deflection (stimulus indicated by arrow; top trace: membrane potential; bottom trace: kymograph of surface deflection). **(d)** Membrane potential pulse (black) and out of plane displacement of the cell surface (red); note: an initial inward movement is followed by expansion.

Chara cells did not lose excitability in the course of plasmolysis. Thus, it was possible to stimulate APs and to study if deflections of the cell surface occur. For this purpose, randomly chosen regions of the protoplast edge were tracked by light microscopy (Fig. 1b). In the absence of electrical stimulation only minor drift of the edge was observed (Fig. S1). In contrast, a distinct surface displacement occurred

---

[*] This process was described previously (28) and resembles a pearling instability that develops at a very slow pace; in the medical/biological literature this phenomenon is sometimes referred to as *beading* or *varicose*. Physically, it is related to the Plateau-Rayleigh instability

upon excitation of an AP (in 142 out of 152 cases; N=30 cells) (Fig. 1c and Video S1 and S2). The maximum deflection was more often outward (95 cases) than inward (47 cases) and typically in the 1—10 µm range (Fig. S1). In the majority of experiments a brief displacement ($\leq$1 s) with opposite directionality preceded the maximum deformation (109 cases; Fig. 1d and Video S2). Such biphasic displacements were also reported in fully turgid cells, albeit with 10—100x lower amplitudes (24). In general, the amplitudes and time courses of the deformations were quite variable at different locations along the protoplast projection edge (Fig. S1). This variation will be explained in a forthcoming manuscript.

Correlation between membrane potential and surface displacement pulse. The AP propagation velocity calculated from the mechanical displacement (8.2±2.4 mm s^{-1}; n=26 pulses in N=4 cells), within experimental accuracy, agreed with that based on the electrical pulse (9.6±2.0 mm s^{-1}; Fig. S2). In most experiments the surface displacement slightly trailed the membrane potential pulse (Fig. 1d). However, since the electrical measurement is by default not as localized as a mechanical measurement, the delay between the electrical and mechanical pulse may be a measurement artifact. Future studies could circumvent this difficulty, for instance, by using fluorescent imaging which allows for localized monitoring of the membrane potential as well. In any case, it was evident that the mechanical deformation outlasted the electrical component (Fig. 1c). The membrane potential pulse in a plasmolysed cell usually had a duration of ~10—20 s, whereas the surface deflection relaxed on timescales that were an order of magnitude longer ($\sim$0.5—5 min). The latter agrees with observations in fully turgid *Charophytes* (23, 24).

Involvement of actin-myosin-motility in surface displacement. Actin and myosin are present in *Characean* cells, but their types and roles differ as compared to muscle cells (29). In *Chara*, coherent sliding of myosin-coated organelles on actin filaments leads to directional streaming of the cytoplasm (velocities up to 100 µm s^{-1}). During an AP, streaming is temporarily arrested and recovers within several minutes (29). This demonstrates that there exists a coupling between membrane excitation and actin-myosin-motility (excitation-cessation-coupling). Furthermore, the relaxation time of cytoplasmic streaming to normal velocities after stoppage (>1min) is of a similar order of magnitude as that of the surface deformation (*cf.* Fig. 1 and Ref. (24)). Thus, stoppage of streaming or a coincident process in the cytoskeleton may be involved in the observed deformations.

We attempted to investigate this possibility. It was reported that membrane excitation can be uncoupled from streaming if extracellular Ca^{2+} is replaced with Mg^{2+} (30). This approach, however, was not feasible, because plasmolysis in the absence of Ca^{2+} led to rupture of the *Chara* cell membrane. In a subsequent series of experiments, cytochalasin D (CytD) was employed. This substance interferes with and arrests cytoplasmic streaming by a presently unknown mechanism (31). Cytochalasins also

uncouple membrane excitation and contraction in muscle cells (*i.e.* the membrane is excitable, but contractility is impaired (32)). Thus, it was expected that treatment with CytD will abolish the cell surface deformation in *Chara* if the latter is dependent on actin-myosin motility. When a *Chara* cell was incubated with CytD, it remained excitable but streaming came to a halt. This is analogous to the effects of CytD on muscle cells. However, when an AP was triggered, the surface deformation of the *Chara* cell persisted (Fig. 2). The time scales of this deflection were similar and the amplitudes were slightly larger as compared to native cells. In combination with observations in muscle cells (32), these results suggest that actin-myosin-motility is not involved in surface deformation during an AP in *Chara*.

Figure 2. Effect of cytochalasin D on surface deflection during an action potential (AP). (top) Displacement of the cell surface upon excitation of an AP in artificial pond water (APW) and **(bottom)** in APW + 50µM cytochalasin D. Stimulus indicated by arrow. Vertical scale bars represent 20 µm.

Micropipette aspiration at rest and during an AP. To better understand the mechanism of the cell surface displacement, micromechanical tests were carried out. A small incision (length ∼500 µm) was made in the cell wall of a plasmolysed *Chara* internode. Through this opening it was possible to directly access the cell surface (see Fig. 1a and Ref. (28)).
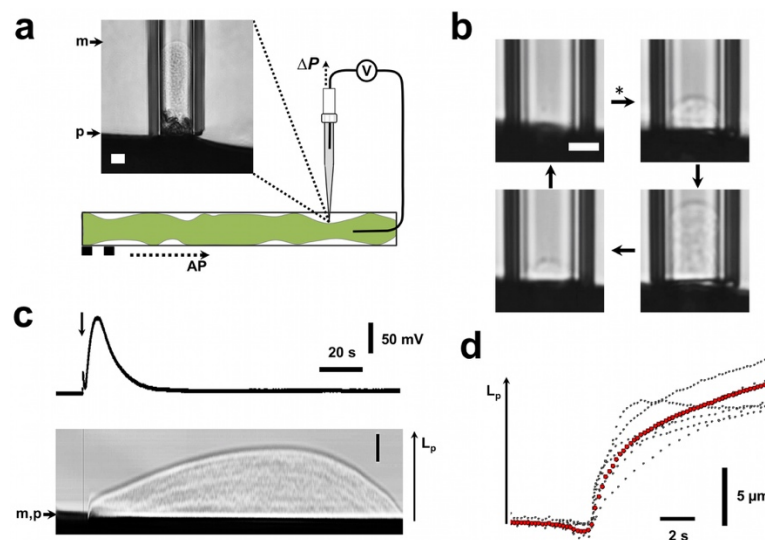
Figure 3. Cell mechanical changes during an action potential (AP). (a) Aspiration of *Chara* cell membrane into a micropipette (membrane projection indicated by ***m***, protoplast surface by ***p***). Note: the cell membrane is peeled off the dense array of chloroplasts (also see Video S3). **(b)** During an AP the membrane underwent a reversible cycle of

motion into and out of the pipette at constant suction pressure. **(c)** Suction pressure (Δp) prior to stimulation of an AP was "clamped" at $0 < \Delta p < \Delta p_{cap}$ (see text for definition of Δp_{cap}). Membrane potential record (top) and aspirated length (L_p; bottom) during an AP. **(d)** Initial phase of membrane motion into pipette (n=6 experiments in N=4 cells; individual traces (black) and average (red)). See text for additional data and statistics. Unlabeled scale bars represent 10 µm.

Micropipette aspiration was used to study the mechanical properties of this surface. For a cylindrical cell that is aspirated into a pipette, the surface tension[†] (σ) is given by the Young-Laplace law

$$\sigma = \Delta p \left(\frac{2}{R_p} - \frac{1}{R_c} \right)^{-1}$$

with Δp the pressure difference between extracellular medium (p_{out}) and pipette (p_p), and R_c and R_p as the radii of the cell cylinder and the pipette respectively (33). The cortical tension of the cell in the resting state σ_{rest} (*i.e.*, before excitation) was determined from the pressure difference (Δp_{cap}) that is required to aspirate a membrane projection with length (L_p) equal to the pipette radius (*i.e.*, when a hemispherical membrane cap was aspirated (34)). In plasmolysed *Chara* cells, σ_{rest} was 0.06 ± 0.01 mN m^{-1} (n=4 experiments in N=3 cells; $\Delta p \sim 10$ N m^{-2}, $R_c \sim 150$ µm, $R_p \sim 10$ µm). This value of membrane tension is in good agreement with that of other excitable systems, for instance, *Nitella* protoplasmic droplets (~ 0.05 mN m^{-1} (35)) and molluscan neurons (~ 0.04 mN m^{-1} (36)).

For aspiration experiments during an AP, the pipette touched the cell surface and a slight suction pressure was applied ($0 < \Delta p < \Delta p_{cap}$; see Fig. 3 and Methods for details). Once the position of the membrane projection within the pipette had remained relatively steady, an AP was stimulated and propagated past the aspiration site. Although the pipette pressure was held constant, L_p increased upon arrival of the AP in all experiments conducted (n=22; N=9 cells; Fig. 3, Video S3). In some cases, a short "inward dip" occurred prior to this movement (Fig. 3d). The membrane projection either moved into the pipette irreversibly (Fig. S3) or reached a maximum and relaxed back to its initial position (Fig. 3c and Video S3). Since cell surface deflections in absence of a pipette were reversible (Fig. 1), it seems likely that irreversibility was a concomitant of the aspiration procedure (37). In general, reversibility prevailed (14 out of 22 cases).

Mechanical analysis of micropipette aspiration during an AP. In a typical aspiration experiment, the surface forces, which are applied by the surface tension σ and the bending rigidity κ, balance the pressure difference between the extracellular medium and the interior of the pipette (Δp). This triplet of surface properties ($\Delta p, \sigma, \kappa$) represents the mechanical state of the system in a 3d-phase space. The

---

[†] For a bilayer membrane that behaves as a closed system: $\sigma = \gamma - \pi$ where γ is the interfacial tension that results from contact of the bilayer with the aqueous environment and π is the surface pressure in the membrane plane. The natural state of a lipid bilayer is defined as $\gamma = \pi$ in which case σ should vanish. Usually, however, it is nonzero (33).

objective of this section is to identify the conditions under which the balance of forces of a weakly aspirated cell is disrupted, such that the system is progressively aspirated (Fig. 3). This was achieved by calculating the aspiration length (L_p) that minimizes the elastic energy of the cell surface for different values of the mechanical parameters (for details see Eq. (7) in Materials and Methods).

An example of the energy as a function of L_p is provided for three values of the surface tension with the other parameters (Δp and κ) held constant (Fig. 4a). This graph demonstrates the existence of a critical value of σ, that flattens the energy function. From there, an increase of surface tension stabilizes the weakly aspirated state ($L_p = 0$), while a decrease of σ leads to an instability; i.e., L_p increases with time, which means that the cell is aspirated into the pipette.

The phase space of the system consists of two regimes: one in which the weakly-aspirated state is stable and one where it is not. A state is unstable when the surface tension and bending rigidity are insufficient to balance the pressure difference (34). A 2d-slice in the $\Delta p - \sigma$ plane of the phase-space is depicted in Fig. 4b. Weakly aspirated states are stable below the dashed line (instability line). The estimated resting state of a plasmolysed *Chara* cell is located in this regime and is marked by a grey ellipse. A transition across the line into the unstable regime (from stable $L_p = 0$ to $L_p > 0$) can be induced, for example, by increasing Δp by ~5 N m^{-2}, decreasing σ by ~50% or decreasing κ by 2-3 orders. The effect of the latter is much smaller, and requires a close proximity of the initial state to the instability line. The short inward motion of a weakly aspirated cell at the beginning of an AP (Fig. 3d) may be induced by a parameter change with opposite directionality (i.e., a decrease in Δp or an increase in σ or κ). These findings are in line with a more elaborate calculation conducted for a different domain of the parameter space (37).
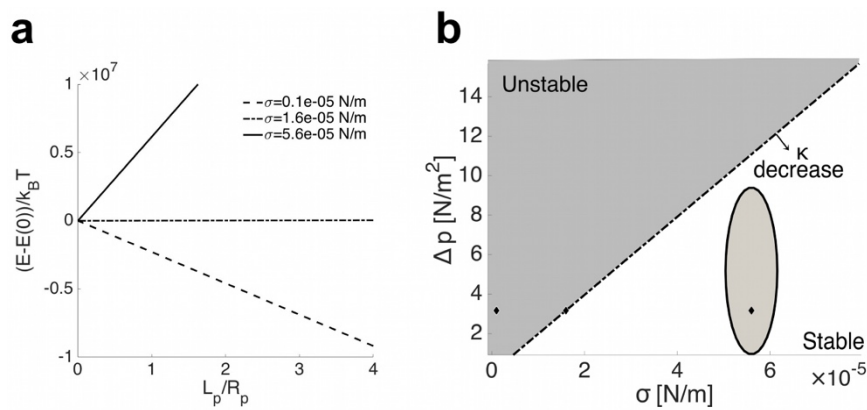
Figure 4. (a) The energy E as a function of aspiration length L_p for three values of the surface tension reveal that the weakly aspired state ($L_p = 0$) can be stable, critical and unstable. Other parameters were held constant: $\kappa = 10^{-19} J$, $\Delta p = 3 \frac{N}{m^2}$, $R_p = 10\ \mu m$ and , $p_p = 6\ bar$. For convenience, the energy was scaled to zero at an aspiration length of zero ($L_p = 0$). In addition, it was normalized by the mean thermal energy at room temperature ($20^o C$), to indicate that the elastic energy stored in the surface is considerably larger. **(b)** The instability line in the Δp–σ phase space. Weakly aspirated states are located below the line. The estimated resting state of the cell is depicted by the grey ellipse (its size represents the experimental error). Decreasing κ effectively shifts the instability line in the direction of the arrow. The three states studied in (a), are depicted as small diamonds in (b).

Discussion

It has been documented by several independent investigators, that APs are accompanied by cellular deformations (4–12, 17, 18, 23, 24). In axons, the latter are typically on the scale of 1—10 nm, whereas in fully turgid *Charophytes* they reach ~100 nm. Herein, it was demonstrated that the actual motions of the cell surface may be 1—2 orders of magnitude larger than these previously reported values. In *Chara*, separation of the plasma membrane from the cell wall reveals micron-sized displacements that were readily observable by light microscopy. These results confirm the assertion that sheathing material and/or cells significantly attenuate mechanical changes at the surface of an excitable cell. In order to better understand the mechanism behind this cellular deformation, micropipette aspiration experiments were carried out. A theoretical analysis of these data indicated that a reversible change in the mechanical properties of the surface (p_{out}, σ, κ) takes place during an AP. This provides a basis to discuss potential mechanism that underlie the cell surface deformation:

Cell surface displacement due to a change in transmembrane pressure. Since hydrostatic pressure does not change during excitation of a cell, significant transmembrane pressure deviations should only arise if the chemical potential of water in the intra- or extracellular space is altered. The chemical potential depends on several parameters that define the thermodynamic phase state of water (temperature, concentration of solutes, etc.). To the best of our knowledge, non-ionic changes of the chemical potential have remained widely unexplored during cellular excitation. It is often assumed that the solute concentration is the most likely parameter to change. Any variations of solute concentration in the intra- or extracellular compartments will lead to a chemical potential gradient for water and thus to a change in osmotic pressure. This gradient will be equilibrated by transfer of water (osmosis) if the membrane is sufficiently permeable. In the classical theory of excitability (the Hodgkin and Huxley model), transmembrane flux of ions is a central mechanism, and cell surface displacements in neurons have been interpreted based on osmosis (38). Others, however, have argued against this assertion (9, 18). A main contradiction emerged from voltage clamp experiments. There, it is assumed that transmembrane flux of ions can be monitored directly in the form of (ionic) currents (21). Ionic currents are low during hyperpolarization (~30 µA cm⁻²) and high during depolarization (~1 mA cm⁻²) (39). If ionic fluxes were the cause of the mechanical response, one would therefore expect larger displacements during depolarization as compared to hyperpolarization. However, the opposite was observed (18). This constitutes a central problem that has to be kept in mind.

In *Chara*, an AP is associated with an efflux of Cl^- and K^+ from the cell ($\sim 3.6 \cdot 10^{-9} \ mol/cm^2$ (40)). Thus, the cell surface may experience a transient osmotic pressure change corresponding to an increase in the extracellular pressure. However, if the efflux of solute is homogenous across the surface, this pressure change will occur inside as well as outside the pipette and thus Δp should remain unchanged. Furthermore, an AP in *Chara* should be followed by a slight decrease of cell volume (25). In the simplest

case, this would lead to a uniform inward movement of the cell surface. Experimentally, however, inward as well as outward deflections were observed (Fig. S1). In combination with arguments by others (9, 18), this underlines that the mechanical changes are not readily explained by ion flux-induced osmosis. In any case, a more detailed consideration of cellular geometry and of the properties of the surface are required.

Cell surface displacements due to changes in surface tension and/or bending rigidity. In a 1945 paper, Hodgkin and Huxley considered several potential mechanisms of the nerve action potential (41). One implied a cooperative change of orientation of lipid dipoles. This possibility was rejected, because such a process should notably alter the electrical membrane capacitance (C_m) – a parameter that at that time was assumed to be constant during an AP. In subsequent studies, it was demonstrated, however, that the assumption of constancy of C_m had been premature (42). This may have led to misinterpretations, for example, because dynamic capacitive currents were ruled out in the original works (2). Based on this point and others, a criticism of the electrical theory was formulated by Kaufmann (2, 13) and more recently by Heimburg (1, 14). These authors proposed that an AP is a pulse propagating in the quasi 2-dimensional membrane interface. Such a reversible (adiabatic) phenomenon must be associated with transient changes in forces and fluctuations of all thermodynamic observables of the system (electric field, pressure, temperature, surface area etc.). More recently, others have elaborated on this proposition (1, 14, 43–45). It was demonstrated that linear (43) as well as non-linear, self-stabilizing pulses (solitary waves) (44, 45) can be excited in lipid monolayers – the simplest model system of a cell membrane. These pulses indeed manifest in *all* thermodynamic variables (*e.g.* electrical, thermal, optical, etc.) (46–48). This is also the case for APs (3, 4, 12, 15, 18). If one compares the solitary waves in protein-free lipid monolayers at the water-air interface with action potentials, additional similarities exist (threshold, amplitude saturation, etc.). Thus, the thermodynamic theory predicts a lateral pressure pulse (related to the surface tension) as well as a change in mechanical susceptibilities (area compressibility and bending rigidity) during cellular excitation. The biphasic mechanical changes during an AP in *Chara* (Figs. 1—3) may be the consequence of pulse-associated changes in σ and/or κ of the excitable medium. The present analysis of micropipette aspiration results suggests that the observed phenomenology (Fig. 3) could be explained by a sufficient decrease in surface tension by ~50 % and/or bending rigidity by ~2 orders. Such changes are not unrealistic, as a decrease in surface tension by ~10% was demonstrated in lipid monolayer pulses (43) and during phase transitions in lipid bilayers κ can be reduced by 1—2 orders of magnitude (49). For most state changes, however, σ and κ will change *simultaneously*. For example, when a fluid lipid membrane is compressed isothermally into the phase transition regime, the lateral pressure as well as κ increase. In order to understand the particular relations between σ and κ in *Chara*, it will be necessary to obtain state diagrams of the excitable medium. The latter could be the plasma membrane or a more extensive cellular interface. It has been reported, for example, that cellular excitation spreads to the vacuole (21), which indicates that the latter may be the case.

On the relation between the electrical and mechanical events. In *Chara*, the cell surface deformation relaxes on time scales that are roughly an order of magnitude longer than the membrane potential pulse (30—300 sec versus 5—10 sec). The mechanical relaxation time agrees fairly well with the duration of the relative refractory period (> 60 sec at room temperature (50)). Thus, the surface deformation dynamics may reveal information about relaxation of the excitable medium, which is not readily apparent from the membrane potential record. Relaxation of the surface deformation in squid giant axons – which closely coincides with the electrical pulse in native cells – also appears to be prolonged under certain conditions, for instance, upon exposure of the axon to TEA (a treatment which extends the membrane potential pulse in time (11)). An even slower, yet otherwise very similar, mechanical displacement pulse occurs during spreading depression (SD) waves in cortical tissue (20). This similarity is intriguing, because an SD wave involves synchronous activity of millions of cells. The overall phenomenology in *Chara* internodes is also reminiscent of that of muscle fibers where cellular shortening lags behind and outlasts the electrical pulse (19).

In principle, there are three potential relations between the membrane potential pulse and the cellular deformation: *(i)* the mechanical and electrical components are two aspects of the same phenomenon (*i.e.*, they are coupled), but the mechanical component relaxes on longer timescales. From a mathematical point of view, such behavior of variables is common in coupled differential equations. From a physical point of view, a phase shift between two aspects of the same phenomenon is also common, for instance, for particle displacement and pressure in a sound wave. *(ii)* The cell surface deformation is an independent phenomenon triggered by the AP. In that case, it should be possible to induce it in absence of membrane excitation. Up to date, this was neither observed by us nor by others (6, 8, 18, 23, 24). An involvement of actin-myosin contractility, as has been proposed previously for axons (51), is not obvious in *Chara* (*c.f.* Fig. 2). The present work did not address if a volume phase transition in the gel-like "ectoplasm-plasmalemma complex" may be involved (10). For axons, there exists evidence that the cortical cytoskeleton may not be essential for the mechanical pulse (18), as removal of cell cortical filaments resulted in a more pronounced deformation. *(iii)* Finally, the mechanical pulse may consist of two components (one on the timescales of the AP and an additional (triggered) component).

Conclusions

The present work demonstrated that an AP is associated with a significant surface deformation (~1—10 µm) in plasmolysed *Chara* cells. This deformation co-propagates with the electrical signal, is biphasic (69% of cases), reversible and relaxes at a slower rate compared to the membrane potential pulse. Due to the magnitude of the displacements as well as the slow time scales of the pulse, this preparation is

well suited to study the physical origin of cell mechanical changes during excitation. Falsifiable predictions were made concerning the surface property changes (p_{out}, σ, κ) that may be involved. Future work should aim at understanding the coupling between the electrical and the mechanical signal. Finally, it will be important to investigate if interfacial pulses in cell membrane models (lipid monolayer) and action potentials in excitable cells can receive a unified theoretical explanation.

Materials and Methods

Materials. All reagents were purchased from Sigma-Aldrich (St. Louis, MO, USA) and were of analytical purity (≥99%). Glass capillaries were obtained from Sutter Instrument (Novato, CA, USA).

Cell cultivation and storage. *Chara braunii* cells were cultivated in glass aquariums filled with a layer of 2-3 cm of New England forest soil, quartz sand and deionized water. The cells were grown under illumination from an aquarium light (14W, Flora Sun Max Plant Growth, Zoo Med Laboratories Inc., San Luis Obispo, CA, USA) at a 14:10 light:dark cycle at room temperature (~20°C). Prior to use, single internodal cells were stored for a minimum of 12 h in a solution containing 0.1 mM NaCl, 0.1 mM KCl and 0.1 mM CaCl$_2$.

Plasmolysis of Chara internode. A single internodal cell (3-6 cm long) was placed on a plexiglass frame into which compartments (~2 x 5 x 10 mm; h x w x l) had been milled. The bottom of the frame consisted of a glass coverslip. Small extracellular sections (length ~5 mm) of the cell were electrically isolated against each other with vacuum grease (Dow Corning Corporation, Midland, MI, USA). The grease also provided structural support for the cell during plasmolysis. Artificial pond water was added (APW; 1 mM KCl, 1 mM CaCl$_2$, 5 mM HEPES, 110 mM D-sorbitol; pH set to 7.0 with NaOH). This APW was replaced gradually with APW of higher osmolarity (regulated by addition of D-Sorbitol; initial: ~120 mOsm kg^{-1}; final: ~270 mOsm kg^{-1}). Addition of ~0.5% bovine serum albumin to the final APW was crucial to minimize adhesion between aspiration pipette and cell membrane. After an equilibration time of 30-60 min, the plexiglass chamber was fixed on the microscope stage. A waveform generator (Agilent 33250A; Agilent, Santa Clara, CA, USA) in combination with a stimulus isolation unit (SIU5; Grass Technologies, Warwick, RI, USA) was used to trigger APs. The membrane potential in one of the compartments far from (1-5 cm) the stimulation site was monitored by intracellular recording. Deflections of the edge of the cell surface are presented as kymographs. In brief, the intensity profile along a line (see Fig. 1) was extracted from every frame of the video recordings (framerate: 10-40 s^{-1}) and was assembled in ImageJ (Version: 1.46r; http://imagej.nih.gov/ij) using the macro ImageJ Kymograph (by J. Rietdorf and A. Seitz). Brightness and contrast of the final kymographs was adjusted. Prominent features in the intensity profile correspond to cell membrane and protoplast edge respectively (Fig. 1). The latter is particularly contrast rich due to the presence of chloroplasts. The membrane potential recording was temporally synchronized with video microscopy by an LED flash into the optical

path of the inverted microscope (Olympus IX71). The time difference between the membrane potential pulse and the mechanical displacement was calculated by depicting deviations in both signals. The criterion for the time of arrival at the measurement site was defined as a deviation of the signal from baseline by three times the standard deviation of baseline variance.

Micropipette aspiration during an AP. A hypodermic needle was used to make a small incision in the cell wall cylinder of a plasmolysed *Chara* internode (26). The medium in the first compartment was replaced with 150 mM KCl to facilitate membrane potential recording via the K$^+$-anesthesia technique. Glass pipettes were pulled to a needle tip (P-97 micropipette puller; Sutter Instrument, Novato, CA, USA) and were broken after scoring with a second pipette to obtain a flat tip. The pipette was filled with APW and was connected to a water column whose height was regulated by a micromanipulator. The typical technical requirements and procedures for micropipette aspiration can be found in the literature (33, 34). When aspirating the membrane of plasmolysed protoplasts, however, one deals with a less defined cellular geometry. Oftentimes, the convoluted protoplast shapes made it difficult to observe the region in which the aspiration pipette touched the cell membrane (because a lobe of protoplast obscured the initial 10-50 μm of the pipette). In such cases, it was possible to reveal the membrane projection by aspirating it beyond the overlapping region. However, this procedure prolonged the experiment and in general required higher suction pressures. To ensure comparability of the results, we resorted to the following procedure: Care was taken to find a position of the protoplast edge, at which the point of contact between pipette and protoplast surface was directly observable. The pipette was slightly pressed against the membrane and a suction pressure was applied. This pressure was insufficient $0 < \Delta p < \Delta p_{cap}$ to aspirate a membrane projection that is longer than the pipette radius ($i.e., L_p > R_p$). The negative pressure required to meet this condition was in the range of $\sim 10^3$-10^4 mN m^{-2} ($R_p \sim 10\ \mu m$). For measurements of the membrane potential, a Ag/AgCl electrode was looped through the water column into the pipette (PS-2132; 50Hz sample rate; PASCO scientific, Roseville, CA, USA).

Mechanical model of micropipette aspiration. Complex aspiration scenarios have been studied previously (37, 52). However, these works were carried out in a different context, at a different regime of the parameter space and did not directly focus on the question posed herein. During an AP, the aspirated Chara cell does not reach a new stable mechanical state. Thus, our focus is only on identifying the stability conditions for the weakly aspired state (zero aspiration). Such compromise allows the use of a simplified spherical geometry. The model assumptions are: (*i*) only the simplest surface contributions are considered: surface tension (σ) and the linear regime of the bending rigidity (κ) (53). (*ii*) At equilibrium, there are no internal flows in the bulk or along the surface; *i.e.,* statics implies that σ, κ, and Δp are constants[‡]. Their dependence on geometrical factors (*e.g.,* surface area) was neglected, because the focus was on the initiation of the instability and not on determining the final strongly-

---

[‡] In principle, these parameters should be coupled to one another by a state equation.

aspirated state. (*iii*) A simplified geometry of a spherical cell was considered instead of the cell-wall-bounded cylinder, because it allows a rather simple analytic expression of the energy function. The simplification is reasonable because the cell volume is much larger than the aspirated segment, $V_{cell} > 10^6 V_{asp}$. The volume of the sphere was matched to that of a plasmolysed *Chara* cell by setting $R = 10^2 R_p$, with $R_p = 10 \ \mu m$. The model geometry is depicted in Fig. 5, although not to scale (the pipette radius is a hundred times smaller than the cell radius). (*iv*) Changes in cell volume during an AP were neglected since $\frac{\Delta V}{V} \sim 10^{-4}$ (25). (*v*) The pressure inside the pipette p_p was assumed constant, $p_p = 6 \ bar$.
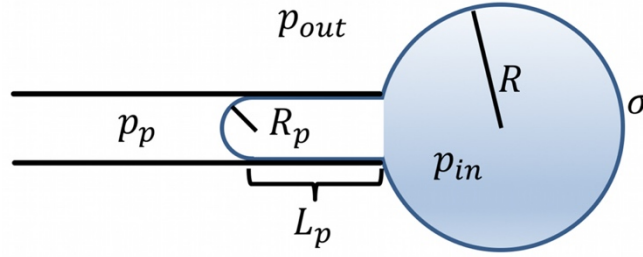
Figure 5. Geometry of the aspiration model (not to scale; in the calculations $R/R_p \sim 10^2$).

The favorable shape was calculated by minimizing the elastic energy function

$$E = \sigma \int dA + \frac{\kappa}{2} \int (2H)^2 dA + p \int dV \quad (1)$$

with A, the surface area, H, the mean curvature of the surface and V, the cell volume. For the simplified geometry considered, the energy function is

$$E = \sigma A + \kappa g_{curv} + p_{out} V_{sph} + p_p V_{asp} - p_{in} V_{tot}. \quad (2)$$

The area and curvature contributions to the energy are respectively

$$A = 2\pi R_p^2 + 2\pi R_p L_p + 2\pi R^2 [1 + \cos(\alpha)], \quad (3)$$

$$g_{curv} = 4\pi \left\{ 4[1 + \cos(\alpha)] + \frac{L_p}{R_p} + 4 \right\}, \quad (4)$$

with

$$\sin(\alpha) \equiv \frac{R_p}{R}. \quad (5)$$

The volume contribution is partitioned into V_{sph} the volume of the part of the cell outside of the pipette (shaded area in Fig. 4a), V_{asp} the volume enclosed in the pipette, and $V_{tot} = V_{sph} + V_{asp}$ (52).

$$V_{sph} = \frac{2\pi}{3} R^3 [1 + \cos(\alpha)] + \frac{\pi}{3} R_p^2 R \cos(\alpha)$$
$$V_{asp} = \frac{2}{3} \pi R_p^3 + \pi R_p^2 \quad (6)$$

The assumption of a constant cell volume simplifies the energy expression into

$$E = \sigma A + \kappa g_{curv} + \Delta p V_{sph} + const, \quad (7)$$

with $\Delta p = p_{out} - p_p$.

Acknowledgements

References

1.	Heimburg T, Jackson AD (2007) On the action potential as a propagating density pulse and the role of anesthetics. *Biophys Rev Lett* 2:57–78.

2.	Kaufmann K (1989) *Action potentials and electromechanical coupling in the macroscopic chiral phospholipid bilayer* (Caruaru, Brazil).

3.	Aidley D (1998) *The physiology of excitable cells* (Cambridge University Press, Cambridge, UK). 4thEd.

4.	Tasaki I, Watanabe A, Sandlin R, Carnay L (1968) Changes in fluorescence, turbidity, and birefringence associated with nerve excitation. *Proc Natl Acad Sci U S A* 61:883–888.

5.	Iwasa K, Tasaki I, Gibbons RC (1980) Swelling of nerve fibers associated with action potentials. *Science* 210:338–339.

6.	Sandlin R, Lerman L, Barry W, Tasaki I (1968) Application of laser interferometry to physiological studies of excitable tissues. *Nature* 217:575--576.

7.	Tasaki I, Iwasa K, Gibbons R (1980) Mechanical changes in crab nerve fibers during action potentials. *Jpn J Physiol* 30:897–905.

8.	Iwasa K, Tasaki I (1980) Mechanical changes in squid giant axons associtated with production of action potentials. *Biochem Biophys Res Commun*:1328–1331.

9.	Tasaki I (1982) *Physiology and electrochemistry of nerve fibers* (Academic Press, New York).

10.	Tasaki I (1999) Evidence for phase transition in nerve fibers, cells and synapses. *Ferroelectrics* 220:305–316.

11.	Tasaki I, Iwasa K (1983) in *Structure and Function in Excitable Cells*, eds Chang D, Tasaki I, Adelman Jr W, Leuchtag H (Plenum Press), pp 307–319.

12.	Tasaki I, Iwasa K (1982) Rapid pressure changes and surface displacements in the squid giant axon associated with production of action potentials. *Jpn J Physiol* 32:69–81.

13.	Kaufmann K (1989) *On the role of the phospholipid bilayer membrane in free energy coupling* (Caruaru, Brazil).

14.	Heimburg T, Jackson AD (2005) On soliton propagation in biomembranes and nerves. *Proc Natl Acad Sci U S A* 102:9790–9795.

15.	Ritchie J, Keynes R (1985) The production and absorption of heat associated with electrical activity in nerve and electric organ. *Q Rev Biophys* 18:451–476.

16.	Wikswo J, Barach J, Freeman J (1980) Magnetic field of a nerve impulse: First measurements. *Science (80-)* 208:53–55.

17.	Hill B, Schubert E, Nokes M, Michelson R (1977) Laser Interferometer Measurement of Changes in Crayfish Axon Diameter Concurrent with Action Potential. *Science (80-)* 196:426–428.

18.	Terakawa S (1985) Potential-dependent variations of the intracellular pressure in the intracellularly perfused squid giant axon. *J Physiol* 369:229–248.

19.	Hodgkin A, Horowicz P (1957) The differential action of hypertonic solutions on the twitch and action potential of muscle fibre. *J Physiol* 136:17P.

20.	Castro GO, Martins-Ferreira H (1970) Deformations and thickness variations accompanying spreading depression in the retina. *J Neurophysiol* 33:891–900.

21. Wayne R (1994) The excitability of plant cells: With a special emphasis on Characean internodal cells. *Bot Rev* 60:265–367.

22. Beilby MJ (2007) Action potential in Charophytes. *Int Rev Cytol* 257:43–82.

23. Kishimoto U, Ohkawa T-A (1966) Shortening of Nitella internode during excitation. *Plant Cell Physiol* 7:493–497.

24. Yao X-C, Rector DM, George JS (2003) Optical lever recording of displacements from activated lobster nerve bundles and Nitella internodes. *Appl Opt* 42:2972–2978.

25. Barry P (1970) Volume flows and pressure changes during an action potential in cells of Chara australis I. Experimental results. *J Membr Biol* 3:313–334.

26. Laver DR (1991) A surgical method for accessing the plasmamembrane of Chara australis. *Protoplasma* 161:79–84.

27. Hayashi T, Kamitsubo E (1959) Plasmolysis in Characeae. *Bot Mag Tokyo* 72:309–315.

28. Foissner I, Wasteneys G (2014) in *International Review of Cell and Molecular Biology*, pp 307–364.

29. Shimmen T (2007) The sliding theory of cytoplasmic streaming: fifty years of progress. *J Plant Res* 120:31–43.

30. Barry W (1968) Coupling of excitation and cessation of cyclosis in Nitella: Role of divalent cations. *J Cell Physiol* 72:153–160.

31. Foissner I, Wasteneys GO (2007) Wide-ranging effects of eight cytochalasins and latrunculin A and B on intracellular motility and actin filament reorganization in characean internodal cells. *Plant Cell Physiol* 48:585–97.

32. Obara K, Yabu H (1994) Effect of cytochalasin B on intestinal smooth muscle cells. *Eur J Pharmacol* 255:139–47.

33. Evans E, Skalak R (1980) *Mechanics and Thermodynamics of Biomembranes* (CRC Press, Boca Raton, FL).

34. Hochmuth RM (2000) Micropipette aspiration of living cells. *J Biomech* 33:15–22.

35. Ueda T, Muratsugu M, Inoue I, Kobatake Y (1974) Structural changes of excitable membrane formed on the surface of protoplasmic drops isolated from Nitella. *J Membr Biol* 18:177–186.

36. Dai J, Sheetz M, Wan X, Morris C (1998) Membrane tension in swelling and shrinking molluscan neurons. *J Neurosci* 18:6681–6692.

37. Chen JZY (2012) Structure of a micropipette-aspirated vesicle determined from the bending-energy model. *Phys Rev E - Stat Nonlinear, Soft Matter Phys* 86:41904.

38. Kim G, Kosterin P, Obaid A, Salzberg B (2007) A mechanical spike accompanies the action potential in mammalian nerve terminals. *Biophys J* 92:3122–3129.

39. Hille B (1992) *Ion channels of excitable membranes* (Sinauer). 2nd Ed.

40. Oda K (1976) Simultaneous recording of potassium and chloride effluxes during an action potential in Chara corallina. *Plant Cell Physiol* 17:1085–1088.

41. Hodgkin AL, Huxley AF (1945) Resting and action potentials in single nerve fibres. *J Physiol* 104:176–195.

42. Takashima S (1979) Admittance change of squid axon during action potentials. *Biophys J* 26:133–142.

43. Griesbauer J, Bössinger S, Wixforth A, Schneider M (2012) Propagation of 2D pressure pulses in lipid monolayers and its possible implications for biology. *Phys Rev Lett* 108:198103.

44. Shrivastava S, Schneider MF (2014) Evidence for two-dimensional solitary sound waves in a lipid controlled interface and its implications for biological signalling. *J R Soc Interface* 11:20140098.

45. Shrivastava S, Kang KH, Schneider MF (2015) Solitary shock waves and adiabatic phase transition in lipid interfaces and nerves. *Phys Rev E* 91:12715.

46. Shrivastava S, Schneider MF (2013) Opto-Mechanical Coupling in Interfaces under Static and Propagative Conditions and Its Biological Implications. *PLoS One* 8:e67524.

47. Griesbauer J, Bössinger S, Wixforth A, Schneider M (2012) Simultaneously propagating voltage and pressure pulses in lipid monolayers of pork brain and synthetic lipids. *Phys Rev E* 86:61909.

48. Fichtl B, Shrivastava S, Schneider MF (2016) Protons at the speed of sound: Predicting specific

biological signaling from physics. *Sci Rep* 6:22874.

49.   Dimova R (2014) Recent developments in the field of bending rigidity measurements on membranes. *Adv Colloid Interface Sci* 208:225–234.

50.   Blatt F (1974) Temperature dependence of the action potential in Nitella flexilis. *Biochim Biophys Acta (BBA)-Biomembranes* 339:382–389.

51.   Rvachev M (2010) On axoplasmic pressure waves and their possible role in nerve impulse propagation. *Biophys Rev Lett* 5:73–88.

52.   Evans E (1980) Minimum energy analysis of membrane deformation applied to pipet aspiration and surface adhesion of red blood cells. *Biophys J* 30:265–284.

53.   Seifert U (1997) Configurations of fluid membranes and vesicles. *Adv Phys* 46:13–137.

Supporting information

Supporting figures
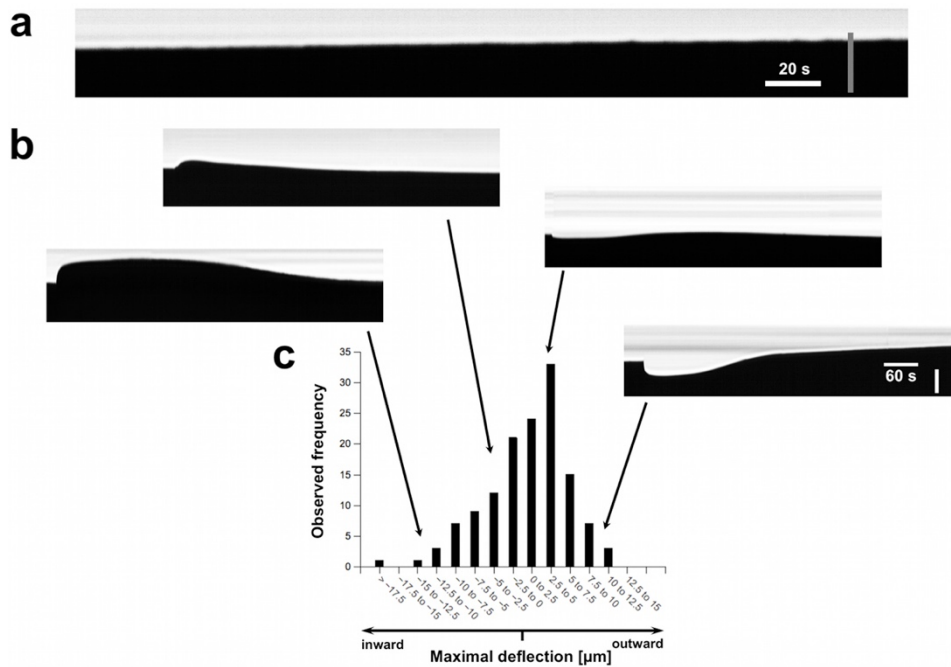
Figure S1. Cell surface deflection during an action potential (AP). (a) Under control conditions (no excitation of an AP) only a slight drift of the protoplast projection edge was observed. A representative kymograph is shown. Vertical scale bar represents 10 µm. Average drift of projection edge during 10 min $\ll 1$µm (n_{total}=134 experiments). **(b)** Upon propagation of an AP across the field of view, the cell surface deflected. At random points on the protoplast, varying amplitudes and directions of the displacement were observed (see kymographs). Horizontal and vertical scale bars apply to all kymographs. The latter represents 10 µm. **(c)** Frequency histogram of maximal displacement of projection edge during an AP (n_{total}=135 experiments in 24 cells).
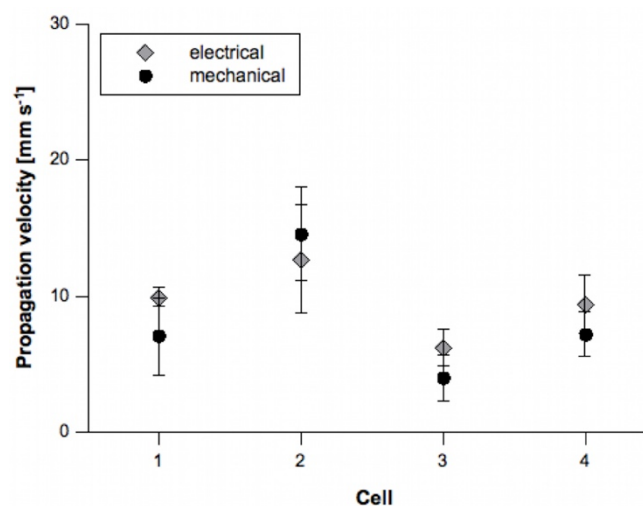
Figure S2. Pulse propagation velocities. Propagation velocity of action potentials in plasmolysed *Chara braunii* internodal cell as calculated from electrical and mechanical component respectively. The plotted values are averages (±standard deviation) of n=6-7 measurements per cell.
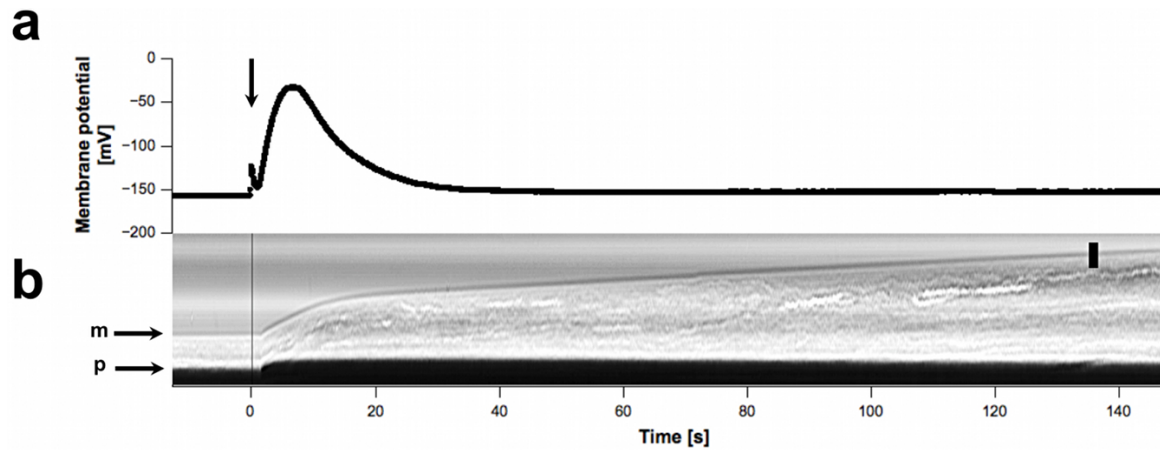
Figure S3. Irreversible membrane aspiration during an AP. An AP was excited under condition $L_p>0$ where the membrane had initially been separated from the protoplast by aspiration (*i.e.* in the unstable regime). **(a)** Recording of membrane potential (arrow indicates stimulus artifact). **(b)** Concurrent with the depolarizing phase of the AP the aspirated membrane (*m*) deflected into the pipette. Kymograph shown is a representative example. See text for detailed statistics. Scale bar represents 10 µm.

Supporting movie legends

Video S1. Cell surface deflection during an action potential (AP). A typical plasmolysed *Chara* cell. The protoplast appears as a dark tube within the cell wall cylinder. Upon stimulation of an AP (9 s mark; ~0.5 cm from observation site), a dynamic deflection of the cell surface occurs (arrows are guides to the eye). Note: biphasic and reversible nature of displacement; transient stoppage of cytoplasmic streaming during AP; field of view ~200 x 110 µm

Video S2. Close-up view of cell surface deflection during an AP. An AP is excited electrically (0.5 s mark; ~2 cm from the observation site). Note: biphasic and reversible nature of the displacement as well as a slight lateral shift of the cell surface; video speed switches from real time to time lapse at 12 s mark; field of view ~35 x 35 µm.

Video S3. Micromechanical testing during an AP. A low suction pressure (insufficient to aspirate the membrane) is applied to a *Chara* cell via a micropipette. This suction pressure is kept constant during the time course of the experiment. When an AP is excited (2.5 s mark), the membrane projection deflects into the pipette. Note: deflection is fully reversible; video speed switches from real time to time lapse at 7 s mark; field of view: ~165 x 90 µm.